Published in final edited form as:

Nat Biotechnol. 2019 June ; 37(6): 667–675. doi:10.1038/s41587-019-0090-6.

Highly efficient expression of circular RNA aptamers in cells using autocatalytic transcripts

Jacob L. Litke[1,2] and **Samie R. Jaffrey**[1,2,*]

[1] Tri-Institutional PhD Program in Chemical Biology, Weill Cornell Medicine, The Rockefeller University, Memorial Sloan Kettering Cancer Center, New York, NY, 10065, USA.

[2] Department of Pharmacology, Weill Cornell Medicine, Cornell University, New York, NY 10065, USA.

Abstract

RNA aptamers and RNA aptamer-based devices can be genetically encoded and expressed in cells to probe and manipulate cellular function. However, their usefulness is limited by low expression and rapid degradation in mammalian cells. Here we describe the Tornado (‘Twister-optimized RNA for durable overexpression’) expression system for rapid RNA circularization, resulting in RNA aptamers with high stability and expression levels. Tornado-expressed transcripts contain an RNA of interest flanked by Twister ribozymes. The ribozymes rapidly undergo autocatalytic cleavage, leaving termini that are ligated by the ubiquitous endogenous RNA ligase RtcB. Using this approach, protein-binding aptamers that otherwise have minimal effects in cells become markedly potent inhibitors of cellular signaling. Additionally, an RNA-based fluorescent metabolite biosensor for *S*-adenosyl methionine (SAM) that is expressed at low levels when expressed as a linear RNA achieves levels sufficient for detection of intracellular SAM dynamics when expressed as a circular RNA. The Tornado expression system thus markedly enhances the utility of RNA-based approaches in mammalian cells.

RNA aptamers are short RNAs that bind intracellular molecules or proteins and can thus modulate intracellular processes[1,2]. Because aptamers can bind specific domains[3] and conformations[4] of proteins, they can either inhibit proteins or modulate their function. Despite their potential applications, RNA aptamers have not achieved nearly the same level of widespread use as other RNA-based technologies such as small interfering RNAs or guide RNAs.

*Corresponding author. srj2003@med.cornell.edu.

Author Contributions S.R.J. and J.L.L. conceived and designed the experiments. J.L.L. carried out experiments and analyzed data. S.R.J. and J.L.L. wrote the manuscript.

Competing Interests

S.R.J, J.L.L., and Weill Cornell Medicine have filed a patent application covering aspects of this technology. S.R.J. is a co-founder of Lucerna Technologies and has equity in this company. Lucerna has licensed commercialization of technology related to Spinach and other RNA–fluorophore complexes.

Data Availability

The authors declare that all data supporting the findings of this study are available within the paper and its supplementary information files.

The major problem with RNA aptamers is that they cannot be expressed at high enough concentrations to efficiently modulate protein function. When expressed using the U6 promoter, the most effective promoter for small RNA expression[5], RNA aptamers achieve concentrations in the low nanomolar range and exhibit half-lives ranging from 0.25 to 1.25 hours[6]. However, proteins are often expressed in the high nanomolar or even micromolar range in cells[7], making aptamer concentrations are too low to stoichiometrically regulate target proteins.

Low expression levels also prevent the use of RNA devices in mammalian cells, such as genetically encoded RNA-based metabolite biosensors. These biosensors are RNA transcripts that comprise a fluorogenic RNA aptamer such as Spinach[8], and an aptamer that binds a metabolite[9–11]. Routine design of these biosensors[12] has enabled fluorescence imaging of diverse metabolites and signaling molecules in bacteria[9–11]. However, unlike bacteria where these RNA-based metabolite biosensors accumulate to micromolar concentrations[9], they are expressed at nanomolar concentrations in mammalian cells[6]. As a result, these biosensors produce undetectable fluorescence signals in mammalian cells.

Here we describe a novel expression system that achieves high-level expression and functional activity of RNA aptamers and RNA devices in mammalian cells. In this approach, RNAs are stable because they are rapidly and efficiently circularized. Circularization is achieved without the co-expression of any additional proteins or enzymes. To trigger RNA circularization, RNA transcripts are expressed containing an RNA of interest flanked by ribozymes that undergo spontaneous autocatalytic cleavage. The resulting RNA contains 5’ and 3’ ends that are then ligated by the nearly ubiquitous endogenous RNA ligase, RtcB. Using this approach, protein-binding RNA aptamers that otherwise have minimal effects in cells become potent inhibitors. Additionally, RNA-based biosensors can now be expressed at high levels and used to detect metabolite fluctuations in mammalian cells. Overall, this expression system enables RNA aptamers and devices to be used as tools for manipulating proteins and imaging cellular processes in mammalian cells.

RESULTS

Designing autocatalytic transcripts as ligation substrates

In order to stabilize RNA aptamers and devices in cells, we wanted to express them as circles. RNA circles are resistant to intracellular exonucleases since they lack a 5’ or 3’ end. Naturally occurring circular RNAs show half-lives that can be measured in days[13], demonstrating the stabilizing effect of circularization.

Endogenous RNA circularization is primarily a consequence of “back-splicing” reactions in mRNA[14,15]. A second mechanism for RNA circularization occurs during tRNA splicing. A subset of tRNAs contain an intron that is cleaved by a tRNA-specific endonuclease[16]. The tRNA endonuclease creates unique ends on RNA: a 5’ hydroxyl and a 2’,3’-cyclic phosphate at the 3’ end[17,18]. These ends are recognized for ligation by RtcB[19]. After cleavage, RtcB ligates the resulting tRNA to form the mature tRNA[20–22].

Since the released intron also contains 5’ and 3’ ends that can be ligated by RtcB, the intron can be circularized (Supplementary Fig. 1a). By inserting the fluorogenic aptamer, Broccoli[23], into the intron sequence of $tRNA^{Tyr}$, we previously showed that a circular Broccoli-containing intron was generated[24].

However in this system, termed “tricY,” circular Broccoli levels were only slightly higher than linear Broccoli expressed from an identical U6 promoter[24]. Based on the high level of uncleaved linear tRNAs (Supplementary Fig. 1b,c), the rate-limiting step appears to be endonucleolytic cleavage to generate RNA fragments with RtcB-compatible ends (Supplementary Fig. 1c).

We therefore wanted to efficiently generate RNAs containing RtcB-compatible 5’ and 3’ ends inside mammalian cells. To mimic processing by tRNA endonuclease, we considered expressing RNA transcripts containing ribozymes that autocatalytically cleave and produce the same 5’ hydroxyl and 2’,3’-cyclic phosphate ends as the tRNA endonuclease.

Most ribozymes show cleavage rates that require tens of minutes or even hours for the cleavage to go to completion in physiological conditions[25]. This would not be useful since an expressed RNA would be degraded before the 5’ and 3’ ends are generated. However, recently described “Twister” ribozymes[26] undergo self-cleavage to produce 5’ hydroxyl and 2’,3’-cylic phosphate ends at rates hundreds of times faster than optimized hammerhead ribozymes[27,28] under physiological conditions[29].

We reasoned that we could genetically encode RNAs containing a 5’ hydroxyl and a 2’,3’-cyclic phosphate by expressing RNAs of interest flanked by Twister ribozymes. After autocatalytic processing, the 5’ and 3’ ends would become substrates for RtcB-mediated ligation. Following ligation the RNA between the ribozymes would be circularized.

In order to distinguish these circular RNA from others derived from backsplicing or tRNA introns, we termed circular RNAs generated in this manner as racRNA, i.e., ribozyme-assisted circular RNA (racRNA) (Fig. 1). The intermediates required to generate the racRNA are designated the primary racRNA (pri-racRNA) and the pre-racRNA, which denote the linear transcript that contains the ribozymes prior to cleavage, and the linear transcripts that are cleaved but not yet circularized (Fig. 1).

Selection of ribozymes for RNA processing

We wanted to test different pairs of ribozymes to see which combinations efficiently process pri-racRNA to pre-racRNA. We first selected potential ribozymes for the 3’ end of the pri-racRNA. After cleavage, a 2’,3’-cyclic phosphate should remain on the pre-racRNA. Since it is important to leave as little residual ribozyme sequence on the pre-racRNA after cleavage, we focused on ribozymes that cleave near its 5’ end, such as the Hatchet ribozyme[30] and a type P1 Twister ribozyme (*O. sativa* Osa-1–4)[31].

We also selected potential ribozymes for the 5’ end of the pri-racRNA. These ribozymes should leave a 5’ hydroxyl on the pre-racRNA. To leave a minimal residual ribozyme sequence, we focused on ribozymes that cleave near its 3’ end, including a type P3 Twister

from *N. vectensis*[26], Twister Sister versions 3 and 4[30], the Pistol ribozyme (M4 construct from *L. sphaericus*)[30] and a minimal type I Hammerhead ribozyme[32].

We wanted the residual fragments left on the 5’ and 3’ ends of the RNA of interest to hybridize to each other in order to juxtapose the 5’ and 3’ ends in a way that resembles the physiologic tRNA substrate for RtcB (Supplementary Fig. 1a). In tRNA, the 5’ and 3’ ends are presented at the ends of a base-paired stem. To mimic this stem in our RNAs, we designed the pre-racRNA so that the 5’ and 3’ ends come together to form a stem comprising 19 base pairs, as well as a 2-nt overhang on the 5’ end and a 7-nt overhang on the 3’ end. The terminal four base pairs of the stem and the overhangs are identical to the ends normally presented by the tyrosine tRNA, a natural substrate for RtcB[21] (Supplementary Fig. 2). In each tested construct, these “stem-forming sequences” at the 5’ and 3’ ends were inserted between each ribozyme’s internal cleavage site and the RNA of interest (Supplementary Fig. 2).

To preserve the ribozymes’ predicted secondary structure after introducing these stem-forming sequences, compensatory mutations were included in each ribozyme sequence (Supplementary Fig. 2). A variant of the P3 Twister was also generated which contains an altered 5’ stem-forming sequence (U2A) to preserve an adenosine that is normally found at this position in this ribozyme (Supplementary Fig. 2).

Next, we synthesized pri-racRNAs with various pairwise combinations of ribozymes by *in vitro* transcription. To facilitate visualization of the RNAs, we used the Broccoli aptamer, which can be readily visualized in gels by staining with DFHBI-1T[6], a fluorophore that becomes fluorescent upon binding Broccoli[23]. In each construct, Broccoli was flanked by the different ribozymes. The cleavage of either or both ribozymes was assessed by examining the size of the RNA (Supplementary Fig. 3). In these experiments, the RNA was resolved by denaturing gel electrophoresis, the denaturant was washed out, and the gel was stained with DFHBI-1T.

Comparison of different pairwise combinations of ribozymes demonstrated that cleavage at both the 5’ and 3’ sides of Broccoli was most efficient when P1 Twister was at the 3’ end, especially when the 5’ ribozyme was a Twister Sister, Pistol ribozyme, or the P3 Twister containing the U2A mutation (Fig. 2a, Supplementary Fig. 3). The hemi-cleaved RNA, i.e., RNA in which either only the 5’ or 3’ ribozyme underwent cleavage, was present at low levels and did not accumulate (Fig. 2a labeled as “5’- or 3’-cleaved”).

We next confirmed that this autocatalytically processed pre-racRNA could be circularized by RtcB. Incubation of the pre-racRNA with RtcB from *E. coli* resulted in a faster migrating band (Fig. 2b), consistent with a known property of circular RNAs[33]. This effect was blocked by incubating the pre-racRNA with T4 polynucleotide kinase, which is expected to generate a 5’ phosphate and convert the 2’,3’-cyclic phosphate to a 3’ hydroxyl[34,35]. Lastly, we treated the RNAs with RNase R, which degrades linear RNA but not circular RNA. Only the RtcB-incubated RNA was resistant to RNase R (Supplementary Fig. 4a).

Overall these data demonstrate an approach for designing transcripts that autocatalytically generate 5’ hydroxyl and 2’,3’-cyclic phosphate ends and can be circularized by RtcB.

Ribozyme-flanked transcripts are circularized in cells

We next tested if ribozyme-flanked aptamers are circularized in cells. We expressed ribozyme-containing transcripts off of a plasmid using a U6 promoter[5]. For each construct, we measured the level and sizes of Broccoli-containing RNA by resolving whole cellular RNA by polyacrylamide gel electrophoresis (PAGE), followed by gel staining with DFHBI-1T. As a preliminary test to determine whether the RNA was circular, we used actinomycin D, which blocks RNA transcription. Typically, linear RNA aptamers are completely lost after 6 hr of actinomycin D treatment due to their rapid degradation[24]. In contrast, circular RNA aptamers should show no change in abundance with this treatment[24].

Transcripts containing a 5' P3 Twister U2A and a 3' P1 Twister showed the highest level of expression of a Broccoli-containing RNA with no detected side-products (Fig 2c, Supplementary Fig. 4b). The abundance of this RNA was unaffected by actinomycin D treatment, suggesting that it is a circular RNA.

We used several approaches to determine whether this abundant and stable Broccoli-containing RNA was a circular RNA. First, we gel purified the band and assessed its sensitivity to RNase R. In contrast to a linear RNA standard, this RNA was not susceptible to RNase R-mediated degradation (Supplementary Fig. 4c).

Second, we found that this stable Broccoli RNA exhibits different mobility in gels with different concentrations of polyacrylamide, which is characteristic of circular RNA[33,36,37] (Supplementary Fig. 5a).

Third, we site-specifically cleaved the RNA using RNase H. RNase H selectively cleaves RNA at sites that are hybridized to a complementary DNA oligonucleotide. If an RNA is linear, then RNase H produces two products. However, if an RNA is circular, then RNase H cleavage produces a single product (Fig. 2d). We expressed Broccoli using Tornado, and purified the resulting putative circular RNA. Incubation of this RNA with RNase H and a 15-nucleotide-long DNA oligonucleotide designed to hybridize to an internal sequence generated a single RNA product. In contrast, a control linear RNA was cleaved into two fragments (Fig. 2d). Together, these experiments show that this stable Broccoli RNA is indeed circular, and not merely an unusually stable linear RNA.

Next, we tested whether there is any heterogeneity at the ligation site in racRNAs. Sequencing of the gel purified racRNAs showed that the ligation site consists of a single sequence (Supplementary Fig. 5b,c) dictated by the two ribozyme-cleavage sites (see Supplementary Fig. 2).

Since this type of racRNA was generated using two Twister ribozymes, we refer to the expression system that generates these circular RNAs as "Tornado" (Twister-optimized RNA for durable overexpression).

Comparison of circular RNA expression methods

We next wanted to compare levels of racRNA generated by the Tornado expression system with other circular RNA expression methods. Expression of linear Broccoli in HEK293T

cells produces very dim green fluorescence (Fig. 3a) at the short exposure time used in this experiment (200 ms). With the same U6 promoter and exposure time, fluorescence was slightly higher in cells expressing Broccoli using the tricY system (Fig. 3a). However, markedly higher levels of green fluorescence were detected when expressing circular Broccoli using the Tornado expression system (Fig. 3a). Notably, the circular RNA was in the cytoplasm, with much lower levels in the nucleus (Supplementary Fig. 6a). Quantification of fluorescence using flow cytometry indicated that cells expressing Broccoli using Tornado were nearly 200 times as bright as linear Broccoli-expressing cells (Supplementary Fig. 6b). These data support the idea that the Tornado expression system produces high levels of circular RNA.

An important question is whether aptamers are folded properly when expressed as a circular RNA. Since Broccoli needs to be folded to produce fluorescence, this experiment demonstrates that circularization does not impair the folding of this aptamer. Furthermore, in-gel fluorescence of linear and circular Broccoli bands suggests that circularization stabilizes the folded form of Broccoli, since Broccoli in a circular RNA exhibits ~50% more fluorescence than linear Broccoli (Fig. 2b).

To further test whether aptamers are folded when expressed using the Tornado system, we expressed Corn, a structurally distinct fluorogenic RNA aptamer that activates the yellow fluorescence of its cognate fluorophore (DFHO)[38]. Expression of Corn as a racRNA resulted in robust fluorescence (Fig. 3b) that was resistant to actinomycin D treatment (Supplementary Fig. 7). In contrast, Corn fluorescence was weakly detected when expressed as a linear RNA, and tricY-expressed Corn transcripts were not detected.

Notably, racRNA can be expressed using the Tornado expression system in all mammalian cells tested (Fig. 3c,d). Thus, the Tornado expression system functions in different cell types and expresses diverse RNA aptamers in functional and folded conformations.

Next, we asked if any other circular RNA expression system generates levels of circular RNA at levels similar to the Tornado expression system. We tested systems previously shown to generate high levels of circular RNA including the rearranged group-I-introns from phage T4[39], the “sno-lncRNA” system which generates nuclear-enriched circular introns[40], as well as the tricY system. We expressed circular Broccoli using each expression system in HEK293T cells. Total RNA was harvested and Broccoli-containing RNA was either not detectable or expressed at markedly lower levels than the level seen with the Tornado system (Fig 3e, Supplementary Fig. 4d). Thus, the Tornado expression system generates substantially higher levels of circular RNA than other expression systems.

Tornado racRNAs achieve micromolar concentrations

We found that the Tornado expression system can result in RNA expression that matches levels of endogenous highly expressed small RNA. SYBR Gold staining of total cellular RNA from HEK293T cells showed the expected abundant cellular RNAs such as tRNA, 5S, and 5.8S RNA (Fig. 3e). Notably, when total RNA was prepared from cells expressing Broccoli using the Tornado expression system, an additional band was detected at nearly equal intensity to the 5.8S and 5S bands and a greater intensity than the tRNA bands. This

band was clearly circular Broccoli, based on its mobility, staining with DFHBI-1T, and its appearance only in cells transfected with Tornado expression system. Thus, Tornado produces circular RNA that reaches similar levels as stable and highly expressed endogenous cellular RNAs.

In many cases, aptamers need to be expressed at levels comparable to protein expression levels to modulate that protein's function. The intracellular concentration of circular Broccoli was therefore determined by generating a standard curve using RtcB-circularized *in vitro* transcribed Broccoli standards (Fig. 3c). Lysates were prepared from a known number of cells, and the average intracellular volume of each cell line was calculated according to its diameter when in suspension (see **Methods**). Based on this analysis, circular Broccoli was 21 μM in HEK293T cells, 16 μM in HeLa cells, and 1.6 μM in HepG2 cells. This indicates that racRNAs are expressed at levels that should saturate protein targets.

racRNA expression is not cytotoxic

We next asked if expressing circular RNAs using the Tornado expression system causes cytotoxicity. Expression of Broccoli using the Tornado expression system elicited low levels of apoptosis, similar to expression of a linear mCherry mRNA, as measured by cleaved poly (ADP-ribose) polymerase (PARP) (Supplementary Fig. 8a). The cellular proliferation rate was also similar (Supplementary Fig. 8b).

Next, we determined if the expression of circular Broccoli activates an innate immunity response, as has been observed for circular RNAs of foreign origin[41]. We measured NF-κB pathway activation and RIG-I levels, which are elevated upon activation of the innate immune pathway[42,43]. NF-κB pathway activation and RIG-I levels were not elevated upon expression of circular Broccoli compared to expression of the mCherry mRNA or linear Broccoli (Supplementary Fig. 9a,b). Overall, these data suggest that innate immune activation by racRNAs is negligible compared to conventional RNA expression systems.

Since racRNA biosynthesis may reduce the availability of RtcB, it is possible that RtcB-dependent tRNA maturation could be impaired. However, northern blotting analysis showed minimal effects on the uncleaved:cleaved ratio of endogenous tRNA substrates of RtcB (Supplementary Fig. 10). Thus, the Tornado expression system does not affect these various measures of cytotoxicity and normal cell function.

Tornado improves the efficacy of protein-inhibiting aptamers

We asked whether expression of protein-binding aptamers using the Tornado system would make them effective protein-modulating agents. Several aptamers have been generated that bind the NF-κB protein monomers, p50 and p65[44–46], preventing their transcriptional activity[47]. These aptamers were expressed as circular RNAs that include the Broccoli aptamer (Fig. 4a) so that aptamer-expressing cells could be detected based on Broccoli fluorescence. Expression of these racRNAs was confirmed by stability to actinomycin D treatment (Supplementary Fig. 11a).

We next assessed whether the racRNAs inhibit NF-κB signaling. In these experiments, NF-κB was activated by application of IL-1β (50 ng/mL, 2.5 h) to HEK293 cells.

Transcriptional activation was measured using a luciferase reporter (see **Methods**). In control cells that expressed circular Broccoli RNA without the NF-κB aptamer, IL-1β induced robust luciferase activity (Supplementary Fig. 11b). This was inhibited by BAY11–7082, an NF-κB pathway inhibitor[48]. One of the aptamers (variant 5), previously shown to bind to the p65 dimer with the 11 nM affinity[45], strongly inhibited activation (~65%) (Supplementary Fig. 11b). Additionally, inhibition of pathway activation was diminished when this aptamer was replaced with a low binding affinity mutant (Supplementary Fig. 11b). Thus, we proceeded with further experiments using this aptamer.

Next, we compared the activity of the NF-κB when expressed as a linear RNA or a racRNA. The linear aptamer is degraded by actinomycin D and thae Tornado-expressed aptamer is more abundant and stable (Fig. 4b). Expression of the linear aptamer inhibits pathway activation by only 8%, while the circular aptamer blocks 65% of activation (Fig. 4c). Additionally, after enriching for cells expressing the circular NF-κB aptamers by sorting transfected cells for Broccoli fluorescence, 85% of pathway activation is inhibited (Fig. 4c). We also observed that the circular aptamer was more folded than the linear aptamer through a B_{max} calculation (Supplementary Fig. 12a,b). Thus, expression as racRNAs markedly improves the effectiveness of pathway inhibiting aptamers.

Imaging cellular metabolites using circular RNA

Genetically encoded biosensors can be developed using fluorogenic RNA aptamers, such as Spinach and Broccoli. Typically RNA-based biosensors are constructed by fusing an aptamer that binds the molecule of interest with the fluorogenic aptamer by a transducer stem. In this way, binding of the metabolite leads to folding and fluorescence of the fluorogenic aptamer[9].

Because RNA devices are highly unstable in mammalian cells, they have only been used in bacterial cells[49], many of which can contain high levels of T7 RNA polymerase, thereby ensuring high expression in the bacterial cytosol.

To test if these RNA devices can be used in mammalian cells when circularized by the Tornado system, we expressed an *S*-adenosyl methionine (SAM) biosensor composed of Broccoli and a SAM-binding aptamer derived from a SAM riboswitch[9]. A linear biosensor with a similar sequence has been previously used in *E. coli*[9].

We designed the racRNA so that circularization occurs at the Broccoli base of the Broccoli-SAM aptamer fusion (Fig. 5a). Although the SAM biosensor was previously optimized in the context of a linear RNA[9], we re-optimized the biosensor in the circular RNA context to have the best signal relative to background. For these optimization experiments, we selected four transducers of variable length and sequence (Fig. 5b). These transducers were inserted between Broccoli and the SAM aptamer, expressed in cells, and cellular RNA was harvested. Each of the transducer variants was expressed as a racRNA (Supplementary Fig. 13). The RNAs were resolved by gel electrophoresis and the background fluorescence and SAM-induced fluorescence was measured in the gel by sequentially adding increasing amounts of SAM to the DFHBI staining buffer (Fig. 5c). The biosensor containing the shortest transducer (Transducer 1) exhibited the largest signal relative to background, high

specificity, and rapid kinetics of fluorescence activation by SAM (Supplementary Fig. 14a,b). Therefore, this biosensor was used for detecting SAM in all subsequent experiments.

Next, we expressed the optimized SAM biosensor in HEK293 cells as a linear RNA and as a racRNA. As expected, gel staining of whole cell RNA showed substantially higher expression of the circular SAM biosensor than the linear biosensor (Supplementary Fig. 14c).

We then sought to determine if the SAM biosensor can detect dynamic changes in SAM levels in HEK293 cells. We readily detected Broccoli fluorescence when the biosensor is expressed using Tornado. Cells expressing the linear biosensor have no detectable fluorescence at this exposure time (200 msec) (Supplementary Fig. 14d). Within 30 min after application of cycloleucine, a SAM biosynthesis inhibitor[50], the fluorescence of cells expressing the circular SAM biosensor was noticeably reduced, with a complete loss of fluorescence within 2 hours (Fig. 5d). Cells expressing the Broccoli aptamer as a racRNA without the SAM aptamer showed no change in fluorescence following treatment with cycloleucine (Fig. 5d). Therefore, the reduction of the fluorescence in cells expressing the SAM biosensor reflects a selective effect of cycloleucine on intracellular SAM levels and not a nonspecific effect on Broccoli fluorescence.

Next, we washed out the cycloleucine to see if the drop in intracellular SAM levels was reversible. Following replacement of the media with cycloleucine-free media, the fluorescence levels rapidly increased to levels observed at the beginning of the experiment (Fig. 5d). No change in fluorescence was observed in the cells expressing racRNA Broccoli (Fig. 5d). This demonstrates that the Tornado expression system allows the SAM biosensor to accumulate to a level that is sufficient to image metabolites in mammalian cells.

DISCUSSION

Synthetic RNA biology entails the use of engineered RNA to manipulate and image cellular function. Because RNA aptamers and devices are highly unstable in mammalian cells, these tools are rarely used for synthetic biology applications in mammalian cells. We show that this problem is overcome by the Tornado expression system which expresses RNA in the form of a circle without the need for coexpression of any proteins. The resulting circular RNAs are highly stable and achieve remarkably high expression levels in cells, comparable to the levels of proteins and the most abundant endogenous small RNAs in cells. The Tornado expression system involves expressing RNAs that contain Twister ribozymes flanking an RNA sequence of interest. This transcript autocatalytically processes itself to become a substrate for RtcB, an endogenous and nearly ubiquitous RNA ligase detected in nearly all animals, bacteria, and archaea[20–22]. The RNA then undergoes end-to-end ligation, resulting in efficient expression of highly stable circular RNA.

Tornado-expressed racRNA aptamers show efficient inhibition of their target proteins. Additionally, RNA-based metabolite biosensors that could only previously be used in bacteria, can now be used in mammalian cells to image metabolite dynamics. We expect that

the Tornado expression system will markedly facilitate the use of diverse aptamer technologies and RNA-based devices in mammalian cells.

Most endogenous circular RNAs are generated by back-splicing, a process that involves the mRNA splicing machinery[14,15]. In contrast, the Tornado expression system represents – to our knowledge – a novel strategy for generating circular RNA.

Circularization is facilitated by hybridization of the pre-racRNA ends, which places the 5' and 3' ends near each other for RtcB-mediated ligation via a stem that forms by hybridization of the 5' and 3' ends of the pre-racRNA. The stem is designed to be relatively short to prevent activation of endogenous double-stranded RNA-detection pathways. Expression of RNAs using the Tornado expression sequence will optimally contain this additional sequence which facilitates RtcB-mediated ligation.

Although longer circular RNAs have been variably observed in the nucleus or cytoplasm[15,51,52], we readily detected racRNAs in the cytoplasm, based on the fluorescence of the circular fluorogenic aptamers. The small size of racRNAs may allow them to pass through the nuclear pores and enter the cytoplasm. Thus, racRNA expression may be useful for manipulating or imaging cytosolic processes.

The Tornado expression system should enable RNA-based tools generated by SELEX[1,2] to be used to manipulate mammalian cells. The high level expression of circular RNAs using the Tornado expression system may make them especially effective for sponging microRNAs[53]. Since, circular RNAs can be templates for translation in cells[54,55], the high level expression described here may markedly enhance the protein synthesis levels achieved using this approach. For any circle synthesized using the Pol III promoter described here, internal U-rich Pol III termination sequences need to be avoided to ensure transcription of the full-length RNA.

Although the circular RNA expressed here did not exhibit cytotoxicity, circular RNAs that contain binding sites for an important RNA-binding protein or microRNA could elicit a cytotoxic response by sequestering these biomolecules. Although racRNAs could be used for therapeutic applications, further studies will be required to establish if they exhibit toxicity in animals.

ONLINE METHODS

Preparation of RNA and observation of ribozyme cleavage

Double-stranded DNA for in vitro transcription were prepared from single stranded DNA templates (Integrated DNA Technologies) and designed to contain a 5' T7 promoter. Templates were amplified by PCR using *Taq* DNA polymerase (New England Biolabs M02373) or Phusion® High-Fidelity DNA Polymerase (New England Biolabs M0530) and checked for quality using 0.8% agarose gel electrophoresis. Impure reaction products were isolated by gel excision and purified with the Qiaquick Gel Extraction kit (Qiagen 28704). Pure PCR reactions were purified with the Qiaquick PCR purification kit (Qiagen 28104).

In vitro transcription reactions used the AmpliScribe™ T7-Flash™ transcription kit (Lucigen ASF3507) carried out at 37 °C. For observing ribozyme cleavage, transcription reactions were quenched by adding polyacrylamide gel electrophoresis (PAGE) sample buffer containing urea (ThermoFisher LC6876). Samples were separated using a precast 6% TBE-Urea Gel (Life Technologies EC68655), and ran at 270 V in TBE buffer until completion. After staining with SYBR Gold (ThermoFisher S11494) diluted 1:10,000 in TBE buffer, RNA bands were imaged using a ChemiDoc MP (Bio-Rad) with a preset channel (302 nm excitation and 590/110 nm emission).

All other transcription reactions for preparing RNA were incubated overnight. Reactions were treated with RNase-Free DNase I (Lucigen ASF3507) at 37 °C for at least 30 min to remove DNA templates and then 13.3 mM EDTA free of RNases (Sigma Aldrich 03690) and incubated at 75 °C for 10 min. RNA was then purified from reactions using the RNA Clean & Concentrator kit (Zymo Research R1015).

Excision and purification of RNA

After staining of PAGE gels, individual RNA bands were isolated from the gel. Bands were excised from gels and crushed by spinning through Gel Breaker Tubes (IST Engineering, Inc. 3388–100). Samples were incubated in an extraction buffer (10 mM Tris HCl pH 6.8, 300 mM NaCl, 1 mM EDTA, prepared at room temperature) for 1 h at 25 or 37 °C, and after placing samples on dry ice briefly to freeze, they were incubated for an additional 1 h. Remaining gel pieces were removed through Costar SpinX columns (Corning 8161), which was followed by ethanol precipitation.

Reactions of RNA templates with T4 PNK and RtcB

After gel purification of autocatalytically cleaved RNA, 300 pmol were treated with T4 polynucleotide kinase (New England Biolabs M0201) according to the manufacturer's protocol at 37 °C for 30 min and inactivated for 20 min at 65 °C. The products were cleaned by phenol chloroform extraction using heavy phase-lock tubes (Quantabio 2302830). 10 pmol of this purified T4-PNK-treated RNA or of the gel purified RNA was ligated using RtcB Ligase (New England Biolabs M0458) for 1 h at 37 °C.

Cloning of autocatalytic circRNA constructs

DNA templates containing Broccoli and each of the ribozyme combinations were prepared as described above with flanking SalI and XbaI restriction sites. Designed using SnapGene software (GSL Biotech), these constructs were cloned downstream of a U6+27 promoter and upstream of the U6 terminator in a pAV vector that contains the SV40 origin[56]. This U6 promoter includes the first 27 nucleotides of U6 RNA as described previously. Subsequent plasmids were made in the same way for cloning one or two aptamers directly into the Tornado expression cassette at NotI and SacII, RsrII, or KflI restriction enzyme sites. A gene for mCherry fluorescent protein expression was introduced into the backbone of this vector.

Cell culture and transfection

HEK293T/17 (ATCC CRL-11268), COS-7 (ATCC CRL-1651), Hep G2 (ATCC HB-8065), and HeLa (ATCC CCL-2) cells were maintained in 1× DMEM (Life Technologies 11995–

065) with 10% FBS, 100 U/ml penicillin and 100 μg/ml of streptomycin under standard tissue culture conditions. NF-κB reporter (luciferase) HEK293 (BPS Biosciences 60650) cells were maintained in these conditions with 50 μg/mL hygromycin B (Life Technologies 10687010). All cells were split using TrypLE Express (Life Technologies) according to manufacturer's instructions.

Cell lines were plated for transfection using FuGENE HD (Promega 2311) according to the manufacturer's instructions using OptiMEM™ I Reduced Serum Media (Thermo Fisher 31985).

For experiments testing the stability of circRNAs, 5 μg/mL actinomycin D (Sigma Aldrich A9415) was added to cells for 6 h prior to extraction of RNA.

RNA extraction

RNA was harvested from cultured cells by removing media and detaching enzymatically or directly lifting cells with 1x Phosphate Buffered Saline (PBS) (ThermoFisher 10010031). Cell suspensions were mixed with TRIzol™ LS Reagent (Invitrogen 10296010), then frozen and store at −20 °C or purified immediately according to the manufacturer's instructions.

Total RNA concentrations were normalized using a NanoDrop 2000 (Thermo Scientific)

In-gel Broccoli imaging

Total RNA (1.0–2.5 μg) were separated using precast 6% or 10% TBE-Urea Gels (Life Technologies EC68655), and ran at 270 V in TBE buffer until completion. Gels were washed and probed for Broccoli as previously described[57], using minimal volumes (15 mL) to reduce escape of RNA from the gel. Gels were washed 3× 5 min with water and then stained for 30 min in 10 μM DFHBI in buffer prepared at room temperature containing 40 mM HEPES pH 7.4, 100 mM KCl, 1 mM $MgCl_2$. Broccoli bands were then imaged using a ChemiDoc MP (Bio-Rad) with 470/30 nm excitation and 532/28 nm emission. Gels were washed additionally with water and stained with SYBR Gold (ThermoFisher S11494) diluted in TBE buffer. RNA bands were then imaged using a ChemiDoc MP (Bio-Rad) with a preset channel (302 nm excitation and 590/110 nm emission). Gel bands intensities were quantified in Image Lab 5.0 software (Bio-Rad).

Reactions of circRNA with exoribonuclease

RNA was treated with T4 PNK or RtcB as described above. Products were purified using phenol chloroform extraction as described above. Purified reactions were treated with RNase R (Lucigen RNR07250) as recommended by the manufacturer.

Site-specific circRNA cleavage

We designed a construct using Tornado that would express a 275-nt circRNA containing a series of scrambled RNA sequences as well as Broccoli. We transfected this plasmid into HEK293T cells, then extracted the RNA and purified the band where we observed in-gel Broccoli fluorescence, as described above. We prepared a sample of linear RNA with the same sequence by in vitro transcription and column purification. We also designed a 15-nt

antisense DNA primer (Integrated DNA Technologies) with reverse complementarity for a region of the scrambled RNA sequence. Site-specific cleavage was performed in reactions containing 100 ng of the target RNA, 10 pmol of the antisense primer, RNasin® Ribonuclease Inhibitor (Promega N211A), and 0.5 μL Hybridase™ Thermostable RNase H (Lucigen H39500) in a total volume of 10 μL. Reaction buffer contained 100 mM NaCl, 40 mM Tris-HCl pH 7.7, 4 mM $MgCl_2$, 1 mM DTT, and 0.03% BSA prepared at room temperature. Reactions were incubated at 50 °C for 10 min before adding Hybridase™. Reactions proceeded for 2 h at 42 °C.

Sequencing of expressed racRNAs

RacRNAs were harvested from HEK239T cells with TRIzol™ LS Reagent (Invitrogen 10296010) and purified by excision from denaturing acrylamide gels. Isolated RNAs were reverse transcribed using SuperScript™ III (Thermo Fisher 18080093) and subsequently amplified by *Taq* DNA polymerase (New England Biolabs M02373) using convergent primers. Amplified DNA was visualized as a ladder of bands on agarose gels and specific bands were excised (see Supplementary Fig. 7a). Excised DNA was cloned by TA cloning into the pCR™4-TOPO™ vector (Thermo Fisher K457502), and individual clones were sequenced.

Microscopy and image processing

For imaging cells, we used pre-coated 3.5 cm glass-bottom dishes (MatTek Corporation P35GC-1.5–14-C) or glass-bottom 24-well plates 1.5 (MatTek Corporation P24G-1.5–13-F) that were coated with poly-D-lysine (Cultrex, 3429–100-01) for at least 3 h and rinsed twice in 1x PBS. For imaging cells longer than a few h, these plates and dishes were additionally coated with Cultrex Mouse Laminin I (Thermo Fisher 50948048) for at least 1 h and rinsed twice in 1X PBS. Cells were subcultured onto glass bottom vessels 1–2 d after transfection, depending on the experiment. 30 min before the imaging, the media was changed into FluoroBrite media (Thermo Fisher A1896701) containing 40 μM DFHBI-1T or DFHO (synthesized[38] or Lucerna 500–1mg) and 0.1 μg/mL of Hoechst 33342 (Thermo Fisher H3570). Live-cell fluorescence images were taken with a CoolSnap HQ2 CCD camera through a 20× or 40× air objective mounted on a Nikon Eclipse TE2000-E microscope and analyzed with the NIS-Elements software. Conditions were maintained at 37 °C and 5% CO_2. The filter set used for Broccoli detection was a filter cube with excitation filter 470 ± 20 nm, dichroic mirror 495 nm (long pass), and emission filter 525 ± 25 nm. mCherry was detected using 560 ± 20 nm excitation filter, 585 nm (long pass) dichroic mirror, and 630 ± 37.5nm emission filter. Corn detection used a filter cube with excitation filter 500±12 nm, dichroic mirror 520 nm (long pass), and emission filter 542±13.5 nm. Hoechst-stained nuclei were imaged with 350 ± 25 nm excitation filter, 400 nm (long pass) dichroic mirror, and 460 ± 25 nm emission filter (all filters are from Chroma Technology). Exposure times: 200–500 msec for Broccoli, 200 msec for mCherry and Hoechst. Total cell fluorescence was computed using ImageJ by measuring the total signal in a cell's area and subtracting background, which was measured by multiplying this area by the average background of an untransfected cell.

Flow cytometry comparing Broccoli-expressing cells

Three days after transfection, HEK293T cells were harvested and resuspended in 4% FBS/1x PBS containing 40 μM DFHBI-1T and kept on ice before analysis. Cells were analyzed using a LSRFortessa™ (BD Biosciences). Populations of cells were gated to avoid cell doublets detected by forward and side scattering, followed by gating for live cells by DAPI fluorescence (355 nm excitation and 450/50 nm emission). Untransfected cells were used as a negative control for gating Broccoli fluorescence (488 nm excitation and 530/30 nm emission). Plots were generated using FlowJo software (Tree Star, Inc.).

Comparison of Tornado with other circular RNA expression methods

Broccoli was cloned into other circular RNA generating expression systems. The permuted-intron-exon system based on group I intron splicing was derived from the td T4 bacteriophage gene as previously described[39,58] and driven by the U6+27 promoter. Plasmids generating spliced sno-lncRNA containing Broccoli[40] and tRNA intron circular RNA containing Broccoli[24] were prepared as described previously.

Quantification of intracellular RNA concentrations

HepG2, HeLa, and HEK293T cells were transfected with a plasmid encoding Tornado expression of Broccoli and a pSuperior plasmid for mCherry expression in a 1:1 ratio. After 2 d, cells were suspended using TrypLE. Each cell type was plated for imaging so that transfection efficiency could be quantified by red fluorescence the next day. For each cell suspension, the diameter and cell quantity in each cell line was quantified, and then total RNA was extracted from each using TRIzol LS as described above. We calculated the gross intracellular volume of each sample based on quantification of cell number and diameter (13 μm for 293T, 20 μm for HeLa, and 18 μm for HepG2). The average cellular was calculated with the formula for spherical volume. We then ran 1 μg of each cell line's total RNA by 10% denaturing PAGE and imaged the Broccoli fluorescence in the gel using DFHBI-1T as described above. We quantified the amounts of circular Broccoli loaded on the gel by loading an *in vitro* circularized racRNA standard (0.01 to 100 ng) of the same sequence in adjacent lanes. Then, we calculated the gross amounts of circular Broccoli for each sample and then calculated intracellular concentration. Lastly, we corrected our concentration values for transfection efficiency observations made in each cell line.

Western blots for detection of apoptosis and innate immune response in cells

For detection of apoptosis, HeLa cells were treated with 1 μg/mL of doxorubicin (Sigma Aldrich D1515) 24 h before lysis or transfected using FuGENE HD (Promega 2311) 48 h before lysis. For detection of innate immune response, HeLa cells were transfected with plasmids or RNA using Lipofectamine™ 3000 (Thermo Fisher L300001) 16 h before lysis. Cells were lysed in RIPA buffer (50 mM Tris-HCl, pH 7.4, 150 mM NaCl, 0.1% Triton X-100, 0.5% sodium deoxycholate, 0.1% sodium dodecyl sulfate, 1mM sodium othovandate, 1 mM NaF, prepared at room temperature) containing Halt™ protease and phosphatase inhibitor cocktail (Thermo Fisher 78440) and quantified using Pierce™ BCA Protein Assay Kit (Thermo Fisher 23225). Proteins were separated by PAGE, transferred to PVDF membranes, and blocked using 5% milk in TBS-T for 1 h at RT. For probing

apoptosis and innate immune response, blots were incubated overnight in TBS-T containing 5% BSA at 4 °C with Cleaved PARP (Asp214) XP® Rabbit mAb (Cell Signaling Technology D64E10) and Rig-I Rabbit mAb (Cell Signaling Technology D14G6), respectively. Control blots were incubated with GAPDH Mouse mAb (Cell Signaling Technology 97166). Then, blots were probed using HRP-linked Mouse IgG anitbodies (GE Healthcare NA931V) or Rabbit IgG (GE Healthcare NA9314V) as secondary antibodies, developed using Pierce™ ECL Substrate (Thermo Fisher 32106), and signal was detected using a ChemiDoc MP (Bio-Rad).

Measurement of cell proliferation rates

HEK293T cells were independently transfected with plasmids encoding Broccoli using Tornado or encoding mCherry with FuGENE HD (Promega 2311). 2 d after transfection, cells were subcultured 1:4 and 1:8 onto glass-bottom plates (MatTek Corporation P24G-1.5–13-F). The next day, fluorescent cells in each 1:4 subculture were counted in 4 fields, as well as the number of Hoechst-stained cells Hoechst. After 2 d, the 1:8 subcultures were imaged in the same way. We calculated the number of non-fluorescent cells in each culture and then quantified doubling times of fluorescent and non-fluorescent cells according to the formula for exponential growth.

Northern Blot measurements

RNA was harvested from cells using TRIzol™ LS Reagent (Invitrogen 10296010) and separated by a denaturing 10% acrylamide gel. After overnight transfer to Hybond™ -N+ Membranes (GE Healthcare RPN1210B), endgogenous $tRNA^{Tyr}$ was probed by a biotin-labeled DNA probe complementary to the 5’ of mature $tRNA^{Tyr}$ (Integrated DNA Technologies). Biotin signal was developed on the membranes using the Chemiluminescent Nucleic Acid Detection Module Kit (Thermo Fisher 89880).

Stimulation and detection of NF-κB signaling

HEK293 recombinant cells containing a NF-κB-promoter-driven luciferase reporter (BPS Sciences 60650) were used to detect activation of the NF-κB pathway. Two days after plasmid transfection, cells were transferred to 96-well plates in triplicate for luminescence detection. The next day, we stimulated cells and detected their activation. Chemically inhibited cells were incubated with 50 μM of BAY 11–7082 (Santa Cruz Biotechnology sc-200615) for 30 min. Cells were stimulated with 50 ng/mL Recombinant Human IL-1β (Peprotech 200–01b) for 2.5 h. Luminescence was generated with the One-Glo™ Luciferase Assay System (Promega E6110) as recommended by the manufacturer and detected at 570 (Molecular Devices SpectraMax® L Microplate Reader).

Electrophoretic Mobility Shift Assay for aptamer binding

Binding of NF-κB aptamers with p65 was detected by electrophoretic mobility shift assay. 15 uL samples containing 11 nM of linear or circular NF-κB and Broccoli fusions were prepared with 20 mM Tris-HCl pH 8.0, 50 mM NaCl, 1 mM $MgCl_2$, 10 U of RNaseOUT™ (Invitrogen, 10777–019, prepared at room temperature), 30 ng/μL yeast tRNA, 0.25 μg/μL BSA, 1 mM DTT, 5% glycerol. Samples were titrated with recombinant p65 (OriGene

Technologies, TP320780) from 0.5 to 763 nM. After separation on a 5% polyacrylamide gel containing 0.25x TBE, RNA was transferred to Hybond™ -N+ Membranes (GE Healthcare RPN1210B) and subsequently treated with proteinase K for 1.5 h. Broccoli-containing RNA was detected by hybridization with DNA probes end-labeled by T4 PNK (New England Biolabs M0201) with ATP, [γ–^{32}P] (Perkin Elmer BLU503H) and purified using illustra™ Microspin G-25 Columns (GE Healthcare 27–5325-01). Bands were visualized using a Typhoon Trio (GE Healthcare) and quantified with ImageJ software before linearizing binding curves into Scatchard plots.

Fluorescence assisted cell sorting of mammalian cells

HEK293 recombinant cells containing a NF-κB-promoter-driven luciferase reporter (BPS Sciences 60650) were used to detect NF-κB pathway activation. 48 h after transfection, cells were resuspended in a 4% FBS/ 1x PBS solution containing 40 μM DFHBI-1T and kept on ice until analysis on the BD Influx™ Cell Sorter (BD Biosciences). With untransfected cells as a negative control for Broccoli fluorescence, transfected cells were analyzed and sorted based on their green fluorescence (ex=488 nm, em= 525±50 nm). Processing and analysis of the data was performed in the FlowJo program (Tree Star, Inc.).

Circular SAM biosensor design and in-gel activation

The previously described SAM biosensor uses Spinach, which was replaced with Broccoli, since it is predicted to have a similar overall structure with improved folding in cells[23]. Transducer variants of Broccoli-SAM aptamer fusions were cloned into the pAV-U6+27-Tornado vector for circRNA expression. Two days after transfection of these plasmids and the plasmid for circular Broccoli into HEK293T cells, actinomycin D was added to cells, which were then harvested and the RNA extracted, as described above. Isolated RNAs from cells treated or untreated with actinomycin D were separated using a 6% or 10% denaturing polyacrylamide gel, and the gels were imaged using DFHBI-1T followed by SYBR Gold staining.

We detected activation of the biosensors' fluorescence in a polyacrylamide gel by first staining with standard fluorescence buffer (10 μM DFHBI-1T, 40 mM HEPES pH 7.4, 100 mM KCl, 1 mM $MgCl_2$) prepared at room temperature. After imaging, we then added 1 μM of *S*-adenosyl-methionine (Sigma Aldrich A7007) to the imaging buffer and stained the gels for an additional 30 min and imaging the signal again. This was repeated 3 more times after progressively adjusting *S*-adenosyl-methionine concentrations to 10, 100, and 1000 μM. Transducer variants signals were compared at each concentration after normalizing to the signal for circular Broccoli in each image.

Intracellular SAM imaging and quantification

HEK293T cells were transfected with Tornado plasmids encoding either the circular SAM biosensor with transducer 1 or circular Broccoli. Two days later, these cells were subcultured onto coated glass bottom plates (MatTek Corporation P24G-1.5–13-F) and imaged the next day. Using live cell conditions described above, we imaged cells before and for 3 h after adding cycloleucine (Sigma Aldrich A48105) to 100 mM at 5 min intervals. Then, we withdrew cycloleucine and continued to image cells every 5 min for 3 additional h. ImageJ[59]

was used for processing images and for measure the total cell fluorescence at each time point.

Fluorescence measurements of biosensor fluorescence *in vitro*

Biosensor RNA was transcribed *in vitro* using the AmpliScribe™ T7-Flash™ transcription kit (Lucigen ASF3507) as describe above. RNAs were column purified and diluted to 1 μM in a buffer prepared at room temperature containing 10 μM DFHBI-1T, 100 mM KCl, 0.2 mM $MgCl_2$, 40 mM HEPES, pH 7.4. *S*-adenosyl methionine, *S*-adenosyl homocysteine, adenosine, or methionine (all from Sigma Aldrich) were added to samples at 100 μM and fluorescence signal was measured at RT using a Fluoromax-4C (Horiba Scientific) with 470 nm excitation and 505 nm emission, 5 nm slit widths, and 0.1 s integration time.

To measure biosensor activation rate, the biosensor RNA was prepared to 1 μM in a buffer containing 10 μM DFHBI-1T, 100 mM KCl, 5 mM $MgCl_2$, 40 mM HEPES, pH 7.4 in a constantly stirring cuvette at 37 °C. Fluorescence was collected by kinetics acquisition with 0.2 s integration time and after 1 min of collecting background signal, 100 μM of *S*-adenosyl methionine was quickly added to the cuvette.

Supplementary Material

Refer to Web version on PubMed Central for supplementary material.

Acknowledgements

We thank J. D. Moon and H. Kim of the Jaffrey lab for helpful comments and suggestions. This work was supported by NIH grant R01DA037755 (S.R.J.) and by NIH fellowship F31AI134100 (J.L.L.). Fluorescence assisted cell sorting experiments reported in this publication were supported by the Office of the Director of the National Institutes of Health under Award Number S10OD019986 to Hospital for Special Surgery.

REFERENCES

1. Tuerk C & Gold L Systematic evolution of ligands by exponential enrichment: RNA ligands to bacteriophage T4 DNA polymerase. Science 249, 505–10 (1990). [PubMed: 2200121]
2. Ellington AD & Szostak JW In vitro selection of RNA molecules that bind specific ligands. Nature 346, 818–22 (1990). [PubMed: 1697402]
3. Rentmeister A, Bill A, Wahle T, Walter J & Famulok M RNA aptamers selectively modulate protein recruitment to the cytoplasmic domain of β-secretase BACE1 in vitro. RNA 12, 1650–1660 (2006). [PubMed: 16888322]
4. Kahsai AW et al. Conformationally selective RNA aptamers allosterically modulate the beta2-adrenoceptor. Nat. Chem. Biol 12, 1–11 (2016).
5. Good P et al. Expression of small, therapeutic RNAs in human cell nuclei. Gene Ther. 4, 45–54 (1997). [PubMed: 9068795]
6. Filonov GS, Kam CW, Song W & Jaffrey SR In-Gel Imaging of RNA Processing Using Broccoli Reveals Optimal Aptamer Expression Strategies. Chem. Biol 22, 649–660 (2015). [PubMed: 26000751]
7. Dittmer PJ, Miranda JG, Gorski JA & Palmer AE Genetically encoded sensors to elucidate spatial distribution of cellular zinc. J. Biol. Chem 284, 16289–16297 (2009). [PubMed: 19363034]
8. Paige JS, Wu KY & Jaffrey SR RNA mimics of green fluorescent protein. Science 333, 642–646 (2011). [PubMed: 21798953]
9. Paige JS, Nguyen-Duc T, Song W & Jaffrey SR Fluorescence imaging of cellular metabolites with RNA. Science 335, 1194 (2012). [PubMed: 22403384]

10. Kellenberger CA, Wilson SC, Sales-Lee J & Hammond MC RNA-based fluorescent biosensors for live cell imaging of second messengers cyclic di-GMP and cyclic AMP-GMP. J. Am. Chem. Soc 135, 4906–4909 (2013). [PubMed: 23488798]
11. You M, Litke JL & Jaffrey SR Imaging metabolite dynamics in living cells using a Spinach-based riboswitch. Proc. Natl. Acad. Sci 112, E2756–E2765 (2015). [PubMed: 25964329]
12. Litke JL, You M & Jaffrey SR Developing Fluorogenic Riboswitches for Imaging Metabolite Concentration Dynamics in Bacterial Cells. Methods in Enzymology 572, (2016).
13. Ashwal-Fluss R et al. CircRNA Biogenesis competes with Pre-mRNA splicing. Mol. Cell 56, 55–66 (2014). [PubMed: 25242144]
14. Jeck WR et al. Circular RNAs are abundant, conserved, and associated with ALU repeats. RNA 19, 141–157 (2013). [PubMed: 23249747]
15. Salzman J, Gawad C, Wang PL, Lacayo N & Brown PO Circular RNAs are the predominant transcript isoform from hundreds of human genes in diverse cell types. PLoS One 7, e30733 (2012). [PubMed: 22319583]
16. Otsuka A, de Paolis A & Tocchini-Valentini GP Ribonuclease ‘XlaI,’ an activity from Xenopus laevis oocytes that excises intervening sequences from yeast transfer ribonucleic acid precursors. Mol. Cell. Biol 1, 269–280 (1981). [PubMed: 6765601]
17. Laski FA, Fire AZ, RajBhandary UL & Sharp PA Characterization of tRNA precursor splicing in mammalian extracts. J. Biol. Chem 258, 11974–11980 (1983). [PubMed: 6413507]
18. Filipowicz W & Shatkin AJ Origin of splice junction phosphate in tRNAs processed by HeLa cell extract. Cell 32, 547–557 (1983). [PubMed: 6186399]
19. Tanaka N, Chakravarty AK, Maughan B & Shuman S Novel mechanism of RNA repair by RtcB via sequential 2’,3’- cyclic phosphodiesterase and 3’-phosphate/5’-hydroxyl ligation reactions. J. Biol. Chem 286, 43134–43143 (2011). [PubMed: 22045815]
20. Popow J et al. HSPC117 is the essential subunit of a human tRNA splicing ligase complex. Science 331, 760–4 (2011). [PubMed: 21311021]
21. Tanaka N & Shuman S RtcB is the RNA ligase component of an Escherichia coli RNA repair operon. J. Biol. Chem 286, 7727–7731 (2011). [PubMed: 21224389]
22. Englert M, Sheppard K, Aslanian A, Yates JR & Söll D Archaeal 3’-phosphate RNA splicing ligase characterization identifies the missing component in tRNA maturation. Proc. Natl. Acad. Sci. U. S. A 2–7 (2011). doi:10.1073/pnas.1018307108
23. Filonov GS, Moon JD, Svensen N & Jaffrey SR Broccoli: Rapid selection of an RNA mimic of green fluorescent protein by fluorescence-based selection and directed evolution. J. Am. Chem. Soc 136, 16299–16308 (2014). [PubMed: 25337688]
24. Lu Z et al. Metazoan tRNA introns generate stable circular RNAs in vivo. RNA 21, 1554–1565 (2015). [PubMed: 26194134]
25. Emilsson GM, Nakamura S, Roth A & Breaker RR Ribozyme speed limits. Rna 9, 907–918 (2003). [PubMed: 12869701]
26. Roth A et al. A widespread self-cleaving ribozyme class is revealed by bioinformatics. Nat. Chem. Biol 10, 56–60 (2014). [PubMed: 24240507]
27. Khvorova A, Lescoute A, Westhof E & Jayasena SD Sequence elements outside the hammerhead ribozyme catalytic core enable intracellular activity. Nat. Struct. Biol 10, 708–712 (2003). [PubMed: 12881719]
28. De la Peña M, Gago S & Flores R Peripheral regions of natural hammerhead ribozymes greatly increase their self-cleavage activity. EMBO J. 22, 5561–5570 (2003). [PubMed: 14532128]
29. Canny MD et al. Fast Cleavage Kinetics of a Natural Hammerhead Ribozyme. J. Am. Chem. Soc 126, 10848–10849 (2004). [PubMed: 15339162]
30. Weinberg Z et al. New classes of self-cleaving ribozymes revealed by comparative genomics analysis. Nat. Chem. Biol 11, 606–610 (2015). [PubMed: 26167874]
31. Liu Y, Wilson TJ, McPhee S a & Lilley, D. M. J. Crystal structure and mechanistic investigation of the twister ribozyme. Nat. Chem. Biol 7, 1–7 (2014).
32. Uhlenbeck OC A small catalytic oligoribonucleotide. Nature 328, 596–600 (1987). [PubMed: 2441261]

33. Tabak HF et al. Discrimination between RNA circles, interlocked RNA circles and lariats using two-dimensional polyacrylamide gel electrophoresis. Nucleic Acids Res. 16, 6597–6605 (1988). [PubMed: 2456529]
34. Cameron V & Uhlenbeck OC 3′-Phosphatase Activity in T4 Polynucleotide Kinase. Biochemistry 16, 5120–5126 (1977). [PubMed: 199248]
35. Das U & Shuman S Mechanism of RNA 2′,3′-cyclic phosphate end healing by T4 polynucleotide kinase-phosphatase. Nucleic Acids Res. 41, 355–365 (2013). [PubMed: 23118482]
36. Zaug AJ & Cech TR The intervening sequence excised from the ribosomal RNA precursor of Tetrahymena contains a 5'-terminal guanosine residue not encoded by the DNA. Nucleic Acids Res. 10, 2823–2838 (1982). [PubMed: 7099968]
37. Ruskin B, Krainer AR, Maniatis T & Green MR Excision of an intact intron as a novel lariat structure during pre-mRNA splicing in vitro. Cell 38, 317–331 (1984). [PubMed: 6088074]
38. Song W et al. Imaging RNA polymerase III transcription using a photostable RNA-fluorophore complex. Nat. Chem. Biol 13, 1187–1194 (2017). [PubMed: 28945233]
39. Ares M Synthesis of circular RNA in bacteria and yeast using RNA. 91, 3117–3121 (1994).
40. Yin QF et al. Long Noncoding RNAs with snoRNA Ends. Mol. Cell 48, 219–230 (2012). [PubMed: 22959273]
41. Chen YG et al. Sensing Self and Foreign Circular RNAs by Intron Identity. Mol. Cell 67, 228–238.e5 (2017). [PubMed: 28625551]
42. Yoneyama M et al. The RNA helicase RIG-I has an essential function in double-stranded RNA-induced innate antiviral responses. Nat. Immunol 5, 730–737 (2004). [PubMed: 15208624]
43. Hornung V et al. 5′-Triphosphate RNA is the ligand for RIG-I. Science (80-.). 314, 994–997 (2006).
44. Lebruska LL & Maher LJ Selection and characterization of an RNA decoy for transcription factor NF-kB. Biochemistry 38, 3168–3174 (1999). [PubMed: 10074372]
45. Wurster SE & Maher LJ Selection and characterization of anti-NF-κB p65 RNA aptamers. RNA 14, 1037–1047 (2008). [PubMed: 18426920]
46. Wurster SE & Maher LJ Selections that optimize RNA display in the yeast three-hybrid system. RNA 16, 253–258 (2010). [PubMed: 20008486]
47. Chan R et al. Co-expression of anti-NFκB RNA aptamers and siRNAs leads to maximal suppression of NFκB activity in mammalian cells. Nucleic Acids Res. 34, 1–7 (2006). [PubMed: 16397293]
48. Keller SA, Schattner EJ & Cesarman E Inhibition of NF-kappaB induces apoptosis of KSHV-infected primary effusion lymphoma cells. Blood 96, 2537–42 (2000). [PubMed: 11001908]
49. Strack RL, Song W & Jaffrey SR Using Spinach-based sensors for fluorescence imaging of intracellular metabolites and proteins in living bacteria. Nat. Protoc 9, 146–155 (2013). [PubMed: 24356773]
50. Lombardini JB & Talalay P Formation, functions and regulatory importance of S-adenosyl-l-methionine. Adv. Enzyme Regul 9, 349–384 (1971).
51. Zhang Y et al. Circular intronic long noncoding RNAs. Mol. Cell 51, 792–806 (2013). [PubMed: 24035497]
52. Li Z et al. Exon-intron circular RNAs regulate transcription in the nucleus. Nat. Struct. Mol. Biol 22, 256–264 (2015). [PubMed: 25664725]
53. Hansen TB et al. Natural RNA circles function as efficient microRNA sponges. Nature 495, 384–8 (2013). [PubMed: 23446346]
54. Chen CY & Sarnow P Initiation of protein synthesis by the eukaryotic translational apparatus on circular RNAs. Science 268, 415–7 (1995). [PubMed: 7536344]
55. Wang Y & Wang Z Efficient backsplicing produces translatable circular mRNAs. RNA 21, 172–179 (2015). [PubMed: 25449546]
56. Paul CP, Good PD, Winer I & Engelke DR Effective expression of small interfering RNA in human cells. Nat. Biotechnol 20, 505–508 (2002). [PubMed: 11981566]
57. Filonov GS & Jaffrey SR RNA Imaging with Dimeric Broccoli in Live Bacterial and Mammalian Cells. Curr. Protoc. Chem. Biol 8, 1–28 (2016). [PubMed: 26995352]

58. Umekage S & Kikuchi Y In vitro and in vivo production and purification of circular RNA aptamer. J. Biotechnol 139, 265–72 (2009). [PubMed: 19138712]

59. Schindelin J et al. Fiji: An open-source platform for biological-image analysis. Nat. Methods 9, 676–682 (2012). [PubMed: 22743772]

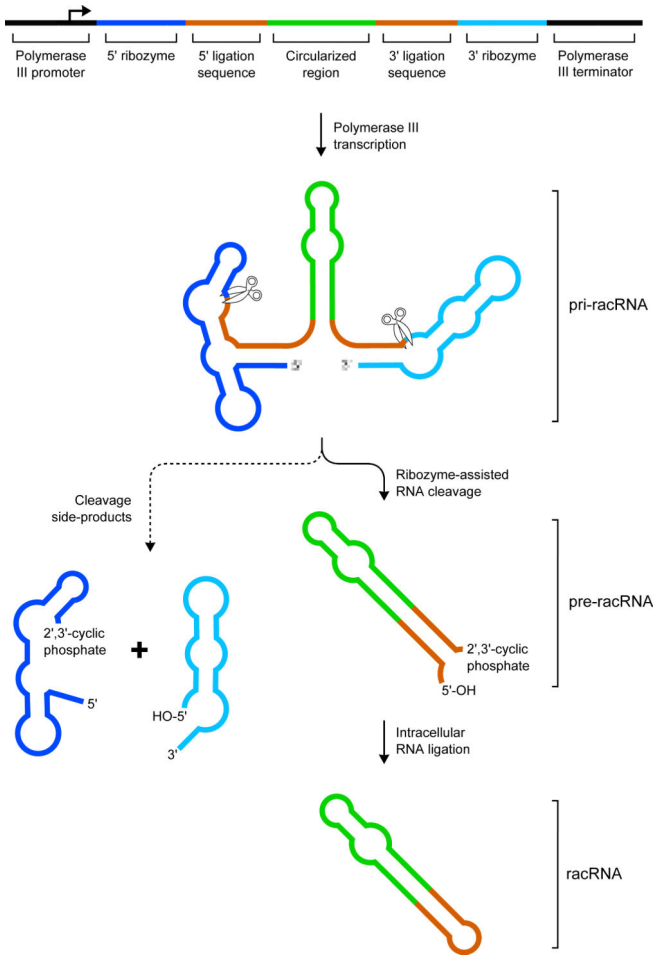

Figure 1. Conceptualization of an autocatalytic circRNA mammalian expression vector.

Construct design for autocatalytically processed circRNA expression. The sequence that becomes expressed as a circular RNA (green) is flanked by the 5’ and 3’-stem-forming sequences (orange), each of which are flanked by the 5’-and 3’-self-cleaving ribozymes (blue and cyan, respectively). Once transcribed, this pri-racRNA becomes cleaved by each ribozyme, which generates a 2’,3’-cyclic phosphate and 5’-OH on the new RNA ends. The stem-forming sequences of the pre-racRNA hybridize and become circularized into racRNA by an endogenous RNA ligase before degradation. The unligated fragments of the pri-racRNA are rapidly degraded by exoribonucleases. Circular RNAs resist endogenous exoribonucleases, allowing the RNA aptamer to reach exceptionally high concentrations.

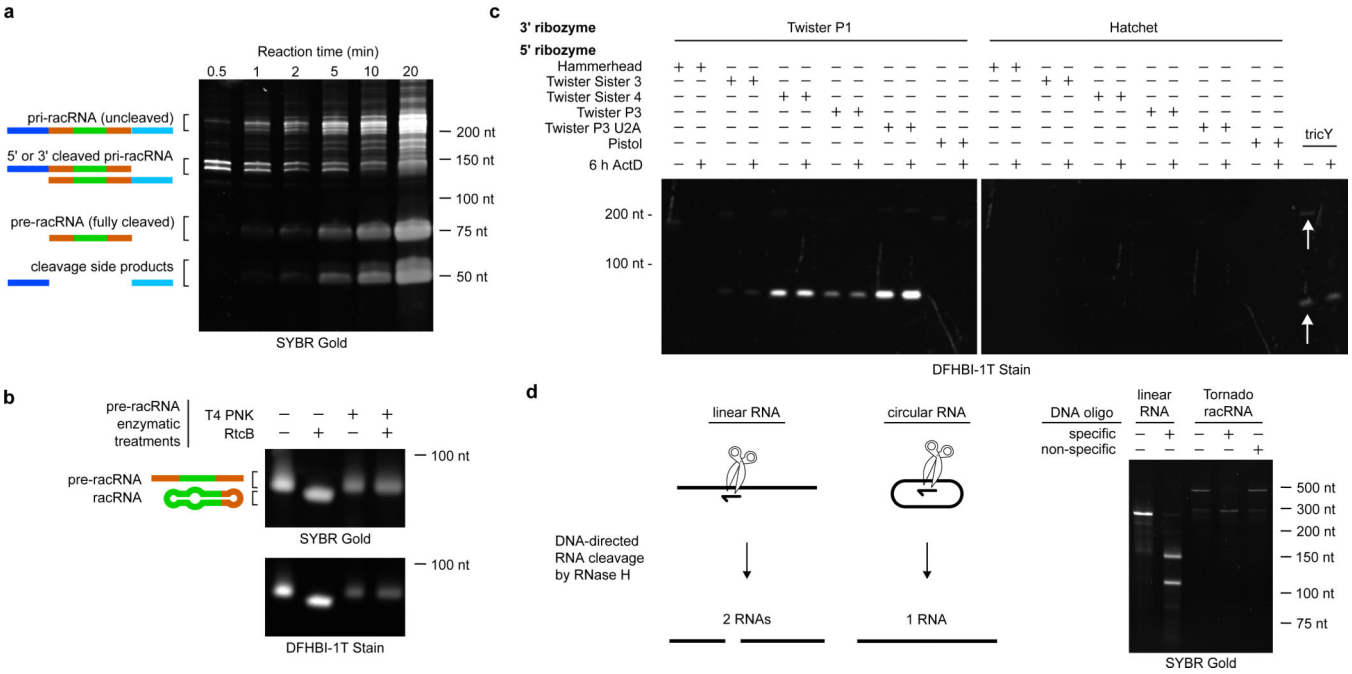

Figure 2. Tornado expression system generates circular RNA

a, Ribozymes efficiently self-cleave during transcription reactions.. The construct containing Twister P1 and Twister P3 U2A ribozymes was transcribed *in vitro* and quenched with urea before running on denaturing PAGE and visualizing RNA. Fully cleaved products and the side products of cleavage accumulate efficiently and rapidly after transcription.

b, Fully-cleaved products of transcription in ***a*** contain appropriate ends for circularization by the endogenous ligase, RtcB. We excised the fully-cleaved RNA from ***a*** and performed an RtcB ligation reactions. RtcB treatment produces a shift in gel mobility that is not observed without ligation or with pre-treatment with T4 PNK. This shift in gel mobility suggests that the fully-cleaved RNA contains the appropriate ends for ligation. Staining of the gel with DFHBI-1T and comparison of fluorescence relative to SYBR Gold signal demonstrates that circular Broccoli is brighter than linear Broccoli.

c, Twister-based ribozyme-assisted circular RNA (racRNA) expression generates significantly higher levels of circular RNA than the previous circular RNA expressing system. HEK293T cells expressed racRNA Broccoli from a variety of racRNA expression systems (see Fig. 1) with different combinations of 5’ and 3’ ribozymes and were compared to expression using the tricY system. Cells were treated with actinomycin D (ActD) for 6 h to observe the drop in RNA levels after new RNA synthesis was inhibited. The Twister P1 and Twister P3 U2A construct, dubbed “Tornado”, expresses high levels of Broccoli RNA that exhibit high stability, characteristic of circRNA.

d, Tornado-expressed RNA is decisively circular. DNA-directed cleavage by RNase H of a linear RNA produces two bands, each of expected size given the transcript length and probe site. The identical treatment of the same sequence expressed from Tornado produces a single band similar in size to the uncleaved transcribed sample.

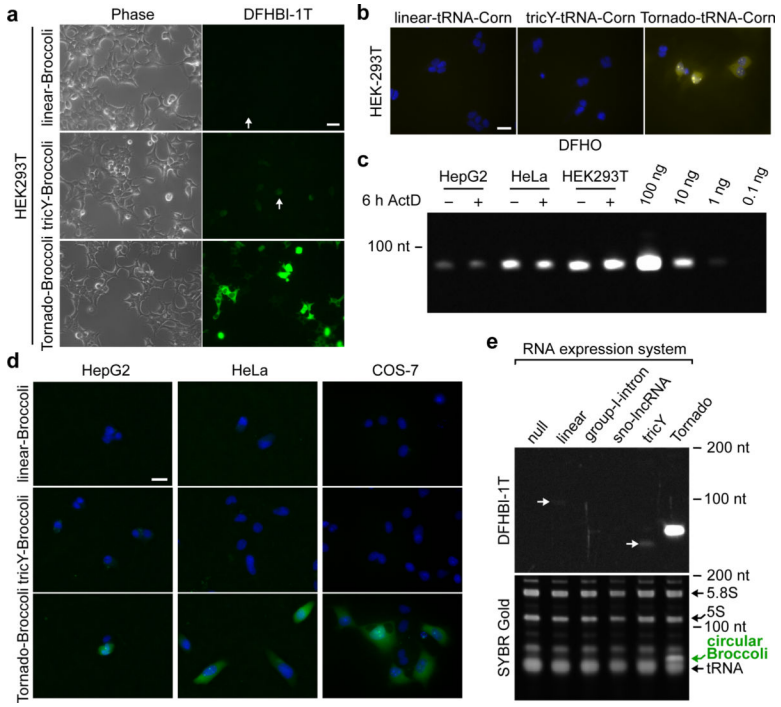

Figure 3. Abundant circRNA expression in different cell lines with fluorogenic aptamers.

a, Broccoli is more readily detected by fluorescence microscopy when expressed as a circular RNA using the Tornado expression system. In HEK293T cells, the Tornado-expressed circular Broccoli signal is readily detected. At the same short exposure time, tricRNA Broccoli exhibits substantially lower fluorescence and linear Broccoli is barely detected. Representative cells showing fluorescence from linear or tricRNA Broccoli are highlighted with white arrows. Scale bar is 25 μm.

b, The Tornado expression system enables efficient expression of the Corn aptamer in a circular form. HEK293T cells expressing Corn in a tRNA scaffold using a linear promoter, the tricY system, and the Tornado expression system were imaged using fluorescence microscopy after incubation of cells with the Corn-binding fluorogenic dye, DFHO. Scale bar is 25 μm.

c, Quantification of Tornado-expressed circular RNA concentration in transfected cells. After three days of expressing Broccoli using Tornado (Tornado-Broccoli), total RNA from HepG2, HeLa, and HEK293T cells were harvested and separated by 10% PAGE alongside circular Broccoli standards (100, 10, 1, 0.1 ng). Normalizing for transfection efficiency, intracellular circular Broccoli concentrations were estimated to 1.6 μM for HepG2, 16 μM for HeLa, and 21 μM for HEK293T cells (see **Methods**).

d, The Tornado expression system results in efficient circularization of an RNA aptamer in a variety of cell lines. Three days after transfection with plasmids encoding linear Broccoli or circular Broccoli with the tricY system or with the Tornado expression system, cells (HepG2, HeLa, and COS-7) were imaged by fluorescence microscopy with DFHBI-1T. Cell nuclei are labeled with Hoechst stain. In all cell types observed, green fluorescence from Broccoli is readily detected only when expressed using the Tornado expression system. Scale bar is 25 μm.

e, Tornado-expressed circular Broccoli is highly abundant. Broccoli was expressed using the Tornade expression system and other methods for generating circular in HEK293T cells. After separation of total RNA on a 6% PAGE gel, Broccoli-containing RNAs are detected by a DFHBI-1T gel stain, while total RNA was detected by SYBR Gold. Circular Broccoli bands are substantially increased when expressed using the Tornado expression system compared to all other methods. The Tornado-generated circular Broccoli band detected by SYBR Gold is as abundant as the 5.8S, 5S, and tRNA bands.

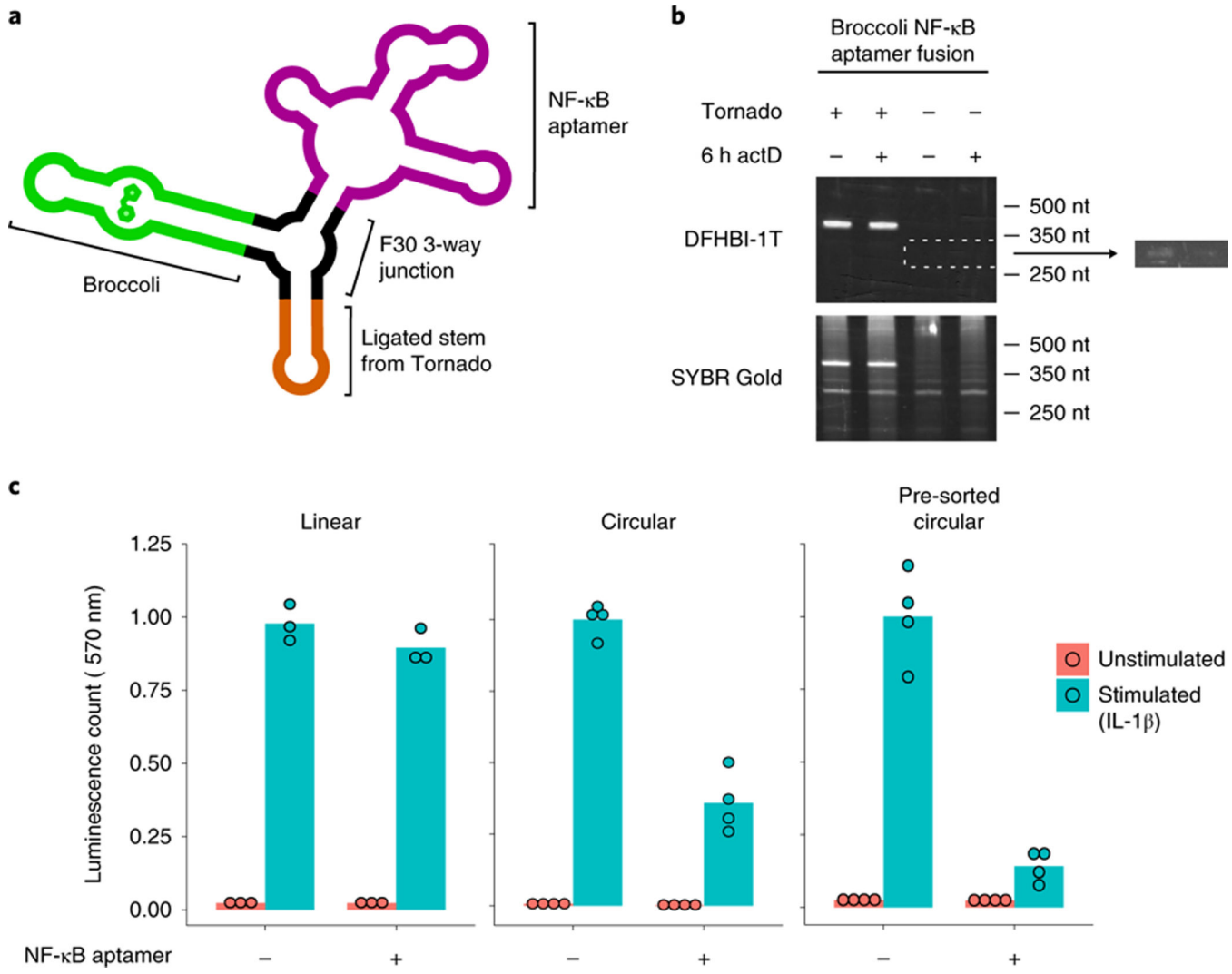

Figure 4. Improved inhibition of NF-κB pathway by circRNA aptamers.

a, Design of circular RNAs that contain NF-κB pathway-inhibiting aptamers. Circular RNAs are designed to contain a F30 3-way junction (black) with Broccoli on one arm, and an NF-κB aptamer on the other arm, while the circularizing stem forms at the base of the F30 3-way junction. This design allows for functional investigation of pathway-inhibiting aptamers while also probing for abundance of this circular RNA using Broccoli fluorescence.

b, Tornado efficiently expresses the NF-κB aptamer as a racRNA in HEK293 cells. HEK293 cells were transfected with a plasmid expressing the NF-κB aptamer as a linear RNA or a a racRNA for two days. Cells were then treated with actinomycin D (ActD) for 6 h and RNA was harvested to detect aptamer expression levels before and after actinomycin D treatment. Aptamer levels were detected based on in-gel staining using DFHBI-1T to detect the Broccoli incorporated into the RNA. The Tornado-expressed racRNA generates a single bright Broccoli-fluorescent bands that is resistant to actinomycin D treatment, while the linear band is barely detected (outlined in white and shown in a brightness-adjusted image on the right).

c, The NF-κB aptamer is an effective pathway inhibitor when expressed using the Tornado expression system. IL-1β-induced NF-κB pathway activation was detected by luminescence in cells encoding luciferase driven by a NF-κB-promoter. Cells expressed either the circular or linear NF-κB aptamer as indicated. IL-1β-induced luminescence is 8% inhibited by linear expression and 70% inhibited by the circular expression. Circular RNA-expressing cells that were pre-sorted for aptamer expression based on their green fluorescence shows more efficient pathway inhibition (~85%). Luminescence was normalized according to the number of cells present during the assay. All signals were normalized to that of the cells expressing RNA without the NF-κB aptamer after activation. Data in this panel represent the mean (n = 3 or 4 stimulation and assay independent samples).

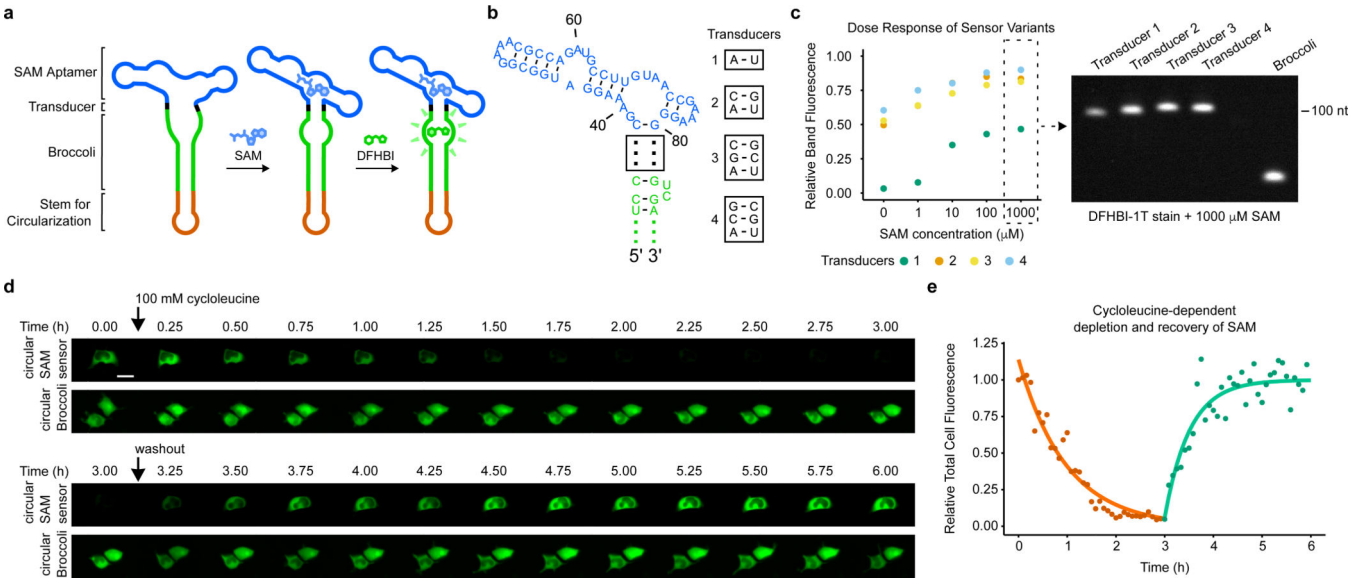

Figure 5. Dynamic SAM detection in mammalian cells by circRNA-based biosensors.

a, Design of intracellular metabolite biosensors composed of circular RNA. Biosensors are designed so that Broccoli folds only when *S*-adenosyl-methionine (SAM) binds to the SAM aptamer. SAM binding to its aptamer leads to folding of the aptamer and stabilization of the transducer stem. The stabilized transducer stem then facilitates Broccoli folding. The SAM biosensor was expressed using the Tornado expression system such that the circularizing stem will be located on the opposite end of Broccoli. This design is adapted from previously reported linear SAM biosensors[9].

b, Sequences of biosensor variants for biosensor optimization. The overall sequence and simplified structure of the SAM aptamer and transducer region is shown. Four different transducer were tested and the sequence of each is shown, boxed.

c, *In vitro* optimization of the SAM biosensor's transducer stem for the SAM detection. RNA from HEK293T cells expressing each biosensor variant using Tornado was harvested, resolved on a PAGE-gel, and then stained with DFHBI-1T to detect RNA bands corresponding to the SAM biosensor. Shown is the quantified fluorescence after adding the indicated concentrations of SAM to the staining solution. Band intensities were normalized to the brightness of the control Broccoli band on the right. Shown is an image of the gel stained with DFHBI-1T along with the highest SAM concentration (1000 μM). The minimal transducer stem (Transducer 1) produced the greatest signal/noise ratio as measured by fluorescence in the presence and absence of SAM.

d, Dynamic detection of intracellular SAM levels using the Tornado-expressed biosensor. HEK293T cells expressing the circular SAM biosensor or circular Broccoli were imaged after treatment with cycloleucine and after replacement of the media with cycloleucine-free media. Images are shown at 15 min intervals along with results for a representative cell. Scale bar is 25 μm.

e, Quantification of live-cell SAM levels based on biosensor fluorescence. Total cell fluorescence from the biosensor was quantified from ***d*** (see **Methods**) at 5 min intervals and plotted after normalizing to the signal from a cell expressing circular Broccoli at the

corresponding time points. SAM decay is observed upon addition of cycloleucine (orange) and SAM recovery (green) is seen after withdrawal of cycloleucine.